

## Strength Development and Microstructural Characterization of Ternary Blended Alkaline Activated Mortars under Different Curing Conditions

[www.doi.org/10.62341/tbam6623](http://www.doi.org/10.62341/tbam6623)

Abduallah Muftah Menshaz\*

Husen Abduallah Alhawat

ammenshaz@elmergib.edu.ly

haalhawat@elmergib.edu.ly

Civil Engineering Department, Faculty of Engineering, Elmergib  
University, Libya

### Abstract:

This article reports the contribution of diverse oxides existent in raw materials such as ultrafine palm oil fuel ash (UPOFA), ground granulated blast furnace slag (GGBFS), and metakaolin (MK) on the performance of alkaline activated mortars (AAMs). The strength and microstructure development of ternary-blended alkali-activated mortar (AATMs) under various curing conditions, namely temperature, ambient, water, and steam were investigated. The mixture was prepared with the same content of binder, aggregate and alkaline activator (AA) and cured at 75 °C for 24 hours. The mixture was characterized in terms of compressive strength (CS) as a main property, and confirmed by XRD, and FTIR analyses. The findings indicated that ternary blended AAMs cured at steam temperatures exhibited higher strengths, accompanied by better compacted and homogeneous microstructure, compared to other curing conditions applied. The results showed that due to the high geopolymerization reactivity of ternary blended alkali-activated mortars which is sensitive to the curing conditions and curing at steam temperature was beneficial to the development of geopolymer CS. The XRD and FTIR analyses showed that the total content of  $Al_2O_3$  and  $SiO_2$  plays an important role in CS development.

**Keywords:** Alkaline activated mortars, Compressive strength, Microstructure, Curing conditions.

## تطوير القوة وتوصيف البنية المجهرية للملاط القلوي المنشط الثلاثي المخلوط تحت ظروف معالجة مختلفة [www.doi.org/10.62341/tbam6623](http://www.doi.org/10.62341/tbam6623)

حسين عبدالله الحوات

عبدالله مفتاح المنشاز\*

haalhawati@elmergib.edu.ly

ammenshaz@elmergib.edu.ly

قسم الهندسة المدنية كلية الهندسة- الخمس جامعة المرقب ليبيا

### الملخص

توضح هذه المقالة مساهمة الأكاسيد المتنوعة الموجودة في المواد الخام مثل رماد وقود زيت النخيل متناهية الصغر (UPOFA)، وخبث الفرن العالي المحبب (GGBFS) و الميكاكولين (MK) في أداء الملاط القلوي المنشط (AAMS). تمت دراسة قوة وتطور البنية المجهرية للملاط المنشط بالقلويات الثلاثية المنحنية في ظل ظروف معالجة مختلفة، وهي درجة الحرارة والهواء والماء والبخار. تم تحضير الخليط بنفس محتوى المادة الرابطة والركام والمنشط القلوي (AA) وتمت معالجته عند درجة حرارة 75 درجة مئوية لمدة 24 ساعة. تم دراسة المخلوط من حيث مقاومة الضغط (CS) كخاصية رئيسية وتم تأكيد ذلك بواسطة تحليلات XRD FTIR. أشارت النتائج إلى أن الملاط الثلاثي المنشط بالقلويات والمعالج في البخار أظهر قوة أعلى، مصحوبة ببنية مجهرية مضغوطة ومتجانسة بشكل أفضل، مقارنة بظروف المعالجة الأخرى المطبقة. أظهرت النتائج أنه نظرًا لتفاعلية البلمرة الجيولوجية العالية للملاط المنشط القلوي المخلوط الثلاثي والذي يكون حساسًا لظروف المعالجة والمعالجة عند درجة حرارة البخار، كان مفيدًا لتطوير الجيوبوليمر CS. أظهرت تحليلات XRD و FTIR أن المحتوى الكلي لـ  $Al_2O_3$  و  $SiO_2$  يلعب دورًا مهمًا في تطوير CS.

الكلمات المفتاحية: ذائف هاون قلوية منشطة، قوة الضغط، البنية المجهرية، ظروف المعالجة.

## 1. Introduction

Construction industry is continuously looking for sustainable alternatives to traditional cement-based products due to their high carbon footprint and environmental impact. Alkaline activated materials (AAMs) have emerged as promising alternatives, offering greater strength, durability, and lower carbon dioxide emissions, in comparison with conventional cementitious materials. Aluminosilicates are a group of naturally occurring and synthetic compounds that contain both aluminum and silicon oxides such as calcined kaolin (metakaolin, (MK) or produced by the industries as wastes including palm oil fuel ash (POFA), and ground granulated blast furnace slag (GGBFS) (Davidovits 2008, Kumar, Kumar et al. 2010). MK is an inorganic material; it is similar to organic materials because it reacts with solid polymers to form a strong aluminosilicate network through polycondensation phase. The inclusion of MK as a precursor material in geopolymers has been found to be very beneficial owing to its natural amorphous phase as well as its small particle size. Meanwhile, millions of tons of a by-product of palm oil, known as POFA are produced every year in several Asian Countries such as Malaysia, Indonesia and Thailand (Tangchirapat, Saeting et al. 2007, Huseien, Ismail et al. 2018). POFA is a by-product of palm oil production that has recently gained attention as a sustainable alternative construction material to traditional cement in construction (Mo, Alengaram et al. 2014). POFA is produced when palm oil waste is burned to generate electricity, and the resulting ash is collected and processed. that has been used as a partial replacement for cement in concrete production POFA is an abundant and low-cost material, rich in a  $\text{SiO}_2$  that can mitigate the environmental concerns generated by large ordinary Portland cement (OPC) production via the synthesis of new binder called geopolymer (Krivenko 1994), besides reducing the high quantity of waste generated from the palm oil industry.

Up to now, most of the available research works were focused on using these materials (MK, and POFA) as singly or binary mixtures, whilst very little research can be found in terms of using ternary precursors in the geopolymer system. Ternary blended alkaline

activated mortars, which include industrial by-products and supplementary cementitious materials, have showed considerable promise in improving the characteristics of AAMs. Understanding the strength development and microstructural characterization of such mortars under various curing conditions is critical for their effective use in sustainable construction practices. Many studies have focused on the factors influencing the microstructure and mechanical performance of geopolymers, with the aim of designing high-performance geopolymer materials. The factors examined have been the effects of molar ratios of different components (Si, Al, Na, and H<sub>2</sub>O ratio) (He, Wang et al. 2016, Yuan, He et al. 2016, Wan, Rao et al. 2017), water content (Lizcano, Gonzalez et al. 2012), particle size (Assi, Deaver et al. 2018), liquid/solid ratio (Liew, Kamarudin et al. 2012), and curing conditions (Fardjaoui, Wicklein et al. 2018, Zhang, Yuan et al. 2021).

Although several studies have been conducted on the strength performance of alkaline-activated ternary blended contains UPOFA, GGBFS, and other materials such as MK According to author' knowledge, there is no work in the literature has clearly discussed the influence of various curing conditions on the ternary blended. The present paper aimed at providing valuable insights into the influence of curing conditions on the structure framework by presenting the changes in CS results and structural formation... Therefore, the objective of this study is to explore the strength development of AATM using locally available materials; UPOFA, GGBFS, and MK as binders. The findings of this work can add to the expanding body of information about the strength development and microstructural characterization of ternary blended AAMs.

## 2. Materials and methods

### 2.1 Materials and mixtures preparation

In the current study, three different types of raw materials were used to produce geopolymer mortar namely POFA, POFA was obtained from the Malaysian United Palm Oil industry, MK, and GGBFS were ordered from Associated Kaolin Industries Malaysia, and YTL Cement Technical Center, Pulau Indah, Selangor, Malaysia, respectively. The treatment process of POFA to obtain UPOFA with

excellent physical properties has been achieved by using the method reported by MegatJohari et al.(Megat Johari, Zeyad et al. 2012). The thermal treatment of kaolin at 750 °C for 1 hour to obtain reactive MK was followed as described in the previous research study(Borges, Nunes et al. 2016, Menshaz, Johari et al. 2017). The chemical compositions of the precursors used in this current study were determined using the X-ray fluorescence (XRF) technique as shown in Table 1. It can be noted that POFA and MK contain a high content of silica oxide (about 65%), while calcium oxide represents around 9%. This is not the same scenario with GGBFS, where CaO exhibited the highest level, followed by SiO<sub>2</sub> (36%) and Al<sub>2</sub>O<sub>3</sub> (15%). SiO<sub>2</sub> was also the dominant oxide in MK, followed by Al<sub>2</sub>O<sub>3</sub>. Therefore, the combination of these materials can provide extraordinary mixtures for geopolymers. Similarly, the physical properties were determined using Mastersizer/E for measuring the particle size distributions and surface area, as well as, MicromeriticsAccuPyc 1330 for measuring the specific gravity as presented in Table 2. The collected silica sand was sieved passed through a 1.18 mm and was retained on a 150 µm sieve as described in ASTM C778(Samet and Chaabouni 2004). River sand was estimated to have fineness modulus of 2.8, and a specific gravity of 2.65. The alkaline activator (AA) used was a combination of sodium silicate solution (Na<sub>2</sub>SiO<sub>3</sub>) (which has the SiO<sub>2</sub>/Na<sub>2</sub>O ratio of 2.2 with the compositions as follows of 14.7% Na<sub>2</sub>O, 32.34% SiO<sub>2</sub> and 55.90% H<sub>2</sub>O) and sodium hydroxide (NaOH) in a pellet form. NaOH and Na<sub>2</sub>SiO<sub>3</sub>were purchased from Qrec (Asia) SdnBhd and Centre West Chemicals SdnBhd, respectively. To make NaOH solution (10 M), the pellets of NaOHwere suspended inside water. This is equivalent to 404.04g of pellets per liter of water., therefore, the prepared solution was left to cool down before it could be used. Next, a Na<sub>2</sub>SiO<sub>3</sub> solution was mixed with the 10 M NaOH solution to make the AA solution. The alkaline activators induce a chemical reaction that results in the formation of a three-dimensional network of binder gel. The AA selection was based on the recommendations as per (Mijarsh, Johari et al. 2015).

**TABLE 1. Chemical compositions of the materials using XRF analysis (% by weight)**

Materials	Oxides									LOI
	SiO <sub>2</sub>	Al <sub>2</sub> O <sub>3</sub>	Fe <sub>2</sub> O <sub>3</sub>	CaO	MgO	TiO <sub>2</sub>	K <sub>2</sub> O	P <sub>2</sub> O <sub>5</sub>	N <sub>2</sub> O	
UPOFA	64.596	5.853	4.743	9.301	3.134	0.219	5.217	5.196	0.053	2.510
GGBFS	36.830	14.449	0.396	39.356	3.592	0.402	0.376	0.019	0.059	0.603
MK	58.571	37.716	1.640	0.026	0.485	1.042	2.269	0.124	-	1.140

**TABLE 2. Physical properties of constituent materials**

Properties	Materials		
	UPOFA	GGBFS	MK
Specific gravity	2.61	2.89	2.6
Median particle size d <sub>50</sub> (µm)	1.1	14.2	4.12
Specific surface area (m <sup>2</sup> /g)	1.871	0.485	0.986

## 2.2 Exposing Samples to High Temperature

All proportions needed for producing alkaline activated ternary mortar (AATM) in this study were prepared and calculated according to ACI 211.1-91 (Nataraja and Das 2010), and presented in Table 3. The AA consisted of 10M NaOH (Sodium hydroxide) concentration, its combination with Na<sub>2</sub>SiO<sub>3</sub> (Sodium silicate) expressed as Na<sub>2</sub>SiO<sub>3</sub>/10M NaOH of 2.5 wt. ratio, and AA/ SMs was kept as 0.52 wt. ratio. The additional amount of water (5% by weight of binder) (AA+ SMs) was added (Mijarsh, Johari et al. 2015). For its proportioning, aggregate/binder ratios were taken as 1.5, as per (Mijarsh, Johari et al. 2015). For all designed mixtures prior to mix, all dried ingredients (SMs with aggregate), listed in Table 3, were placed in L5 automatic Hobart N50 mixer, and mixed

first together for 3mins, before adding AA solution. The mixing procedures were conducted as suggested by (Mijarsh, Johari et al. 2015). All cubic specimens with the dimension of 50 x 50 x 50 mm were cast with a prepared mix in double layers wherein every layer was shaken in vibration table for 15 seconds. Then, all moulds were kept at room temperature ( $25 \pm 2^\circ\text{C}/70 \pm 5\%$  relative humidity) for 12 hours. Following that, the samples were de-moulded and wrapped with heat resistant vinyl bags to prevent losing the moisture, and immediately then placed in an oven at  $75^\circ\text{C}$  for 24 hours (Mijarsh, Johari et al. 2015). Finally, the samples were left in ambient conditions ( $25 \pm 2^\circ\text{C}$  and  $70 \pm 5\%$  RH) till the day of testing (i.e., 3, 7, 14 and 28 days).

**TABLE 3. Mixture formulation of AATM ( $\text{kg}/\text{m}^3$ )**

Mix No.	Solid materials			Sand	$\text{Na}_2\text{SiO}_3$	NaOH		Added water
	UPOFA	MK	GGBFS			pellet	water	
AATM	288	205.5	328.8	1230	305	40	80	60

### 2.3 Testing of specimens

The CS of AAMs specimens was tested according to ASTM C109 (C109/C109M 1999) at different ages including 3, 7, 14 and 28 days. The CS for the mix was taken as the average of three of AAMs specimens for each aging test. To aid understanding the mechanisms driving the ternary blended AAMs' strength development, some samples were collected from crushed cubes, and prepared to identify their crystalline phases using X-ray diffraction (XRD), FTIR and TGA analyses. XRD machine set with  $\text{Cu K}\alpha$  radiation of  $1.5406 \text{ \AA}$  was utilized to determine the samples phases by applying  $2\theta$  in the broad peak ranges from  $10^\circ$  to  $80^\circ$ . The diffraction patterns were then analysed using Expert High Score Plus software, while Rietveld refinement method was used to conduct the quantification. Moreover, FTIR analysis was used to identify the different types of chemical bonds in the materials on a

molecular level. The infrared spectra were recorded in the range of 400–4000  $\text{cm}^{-1}$  wave numbers.

### 3. Results and discussions

#### 3.1 Effect of different curing on compressive strength

Figure 1 displays the CS of AATMs at four different types of curing. It can be observed from Figure 1 that alkaline activated mortar cured at ambient temperature recorded the lowest CS at all tested ages, while higher strengths were observed with those cured in water. It is obvious that there were correlation effects of curing conditions at a certain level that cause an increase in CS. However, AAMs samples cured under steam conditions showed the highest 28-day CS, in comparison with those cured in dry environments (i.e., ambient, water, and temperature curing), since steam can have accelerate the geopolymerization process (Huseien, Sam et al. 2019). The change in curing conditions of the ternary binder can result in a clear difference in the content of CaO and  $\text{Al}_2\text{O}_3$ , which in turn influences the development of CS. This can be explained by the higher dissolution of  $\text{Al}_2\text{O}_3$  compared with  $\text{SiO}_2$ , producing a higher rate of condensation (Sharmin, Alengaram et al. 2017). Moreover, the low content of  $\text{Al}_2\text{O}_3$  can cause at the reduction in the CS obtained (Ariffin, Azreen et al. 2011). This might be attributed to the incomplete geopolymerization process. However, the increase in  $\text{SiO}_2$  can cause a negative effect on the strength (Ranjbar, Mehrali et al. 2014), which is linked to the dense gel particles and large interconnecting pore (Duxson, Provis et al. 2005).

The highest CS of the ternary binder was recorded under steam curing, achieving 88.89 MPa. The increase in source of  $\text{Al}_2\text{O}_3$  is linked to the increase in the  $\text{Al}(\text{OH})_4^-$  species in the initial process of reactions occurred with alkaline hydroxides ( $\text{OH}^-$  ions), primarily NaOH, which leads to a faster rate of condensation reaction between the dissolved anions  $\text{SiO}_2(\text{OH})_2^{2-}$ ,  $\text{SiO}(\text{OH})_3^{-1}$  and  $\text{Al}(\text{OH})_4^-$  as well as the network-modifications of  $\text{Ca}^{2+}$ ,  $\text{Na}^+$ , and  $\text{Al}^{3+}$ , causing formation of higher N–A–S–H over C–A–S–H and C–S–H type gels. In other words, the reaction between  $\text{SiO}_2(\text{OH})_2^{2-}$  or  $\text{SiO}(\text{OH})_3^{-1}$ ,  $\text{Al}(\text{OH})_4^-$  and  $\text{Ca}^{2+}$  species as a function of pH in the system continues until all available  $\text{Ca}^{2+}$  ions are exhausted over

time, also decreases the pH due to the consumption of OH<sup>-</sup> ions in the initial reaction. The reduction in pH and OH<sup>-</sup> ions can offer the proper environments that may facilitate the formation of N–A–S–H gel. It was reported that the increase in Al<sub>2</sub>O<sub>3</sub> and CaO causes the rapid setting time of conventional geopolymer systems, but increase in Al<sub>2</sub>O<sub>3</sub> caused detrimental effects of strength results than CaO that reducing the potential detrimental effect on the strength(Stevenson and Sagoe-Crensil 2005, De Silva and Sagoe-Crenstil 2008, Chindaprasirt, De Silva et al. 2012, Tchadjie and Ekolu 2018).

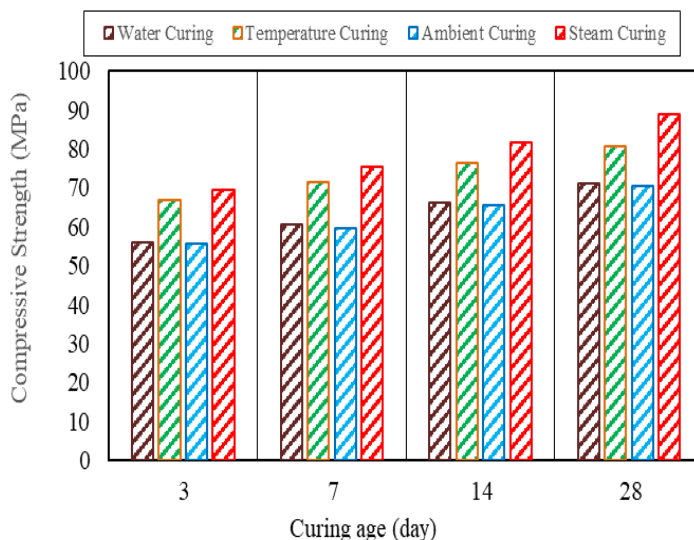


Figure 1. Compressive strengths of AATM samples under different curing conditions.

### 3.2 AAMs phases analysis using X-ray diffraction

As illustrated in Figure 2, the XRD results of AATM mixtures indicated the formation of several phases during the alkaline-activated synthesis. All the XRD diffractograms of AATM showed the presence of crystalline peaks of quartz, albite (N–A–S–H) and anorthite (C–A–S–H), Jadeite (NaAlSi<sub>2</sub>O<sub>6</sub>). The phase of jadeite (NaAlSi<sub>2</sub>O<sub>6</sub>) belongs to aluminosilicate family, and has a single

chain (Si) tetrahedrally-coordinated crystal structure with Na and Al in its octahedral coordination (Kupwade-Patil and Allouche 2012). The formation of N–A–S–H type gel as the main product within the three dimensional network is mainly associated to the presence of MK in the mixture (Granizo, Alonso et al. 2002, Gao, Yu et al. 2015), whilst C–A–S–H gel formed due to the presence of GGBFS with a high Ca content, which contributes to accelerating the rate of activations. These precursors influenced the AATM reactivity due to several factors as the main factors are mineral composition, morphology, and fineness to achieve high performance (Singh, Ishwarya et al. 2015). These results obtained in the current work are in line with those stated by other researchers (Yusuf, Megat Johari et al. 2014). The change in the total content of this material can be confirmed by the change in the peak intensity of crystalline phases as shown in Figure 2. These alterations in the in peak intensity delayed the activation process, strengthened the structure and reduced the mechanical strength of AAMs (Al-Majidi, Lampropoulos et al. 2016).

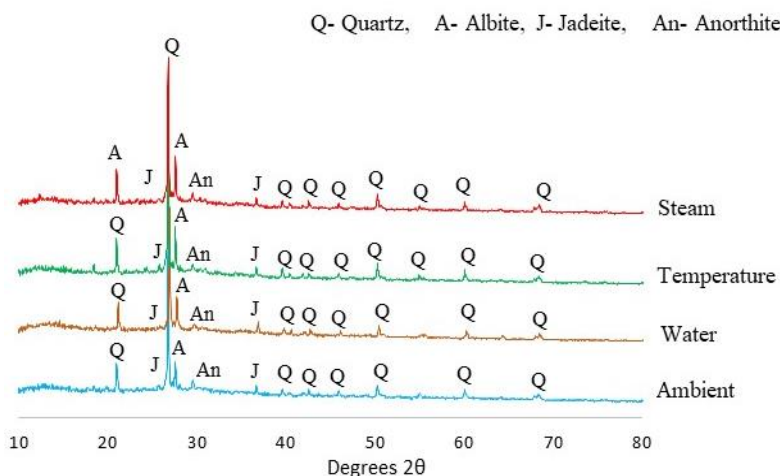


Figure 2. X- ray diffractograms of AATM mixtures at 28 days.

### 3.3 FTIR analysis

Figure 3 illustrates the vibration bands of FTIR analysis for AATMs

at 28 days curing. The FTIR spectra for the various vibration bands shown in the figure confirmed the presence of N–A–S–H, C–S–H and (C–(A)–S–H) gels in the mortars based on the vibrations of Si–O–Si or Si–O–Al and Si–O in plane and bending modes. FTIR is a chemical analysis method used to find the reaction zones of Si–O and Al–O, and identify the degree of geopolymerization and formation of reaction products in the various geopolymer mixtures (García-Lodeiro, Fernández-Jiménez et al. 2010, Mijarsh, Johari et al. 2015).

The current study has focused on specific spectral zones: the bands at 1200–900  $\text{cm}^{-1}$  corresponding to the asymmetric stretching vibration of (Si–O–Si) and (Si–O–Al); the bands assigned around 3468  $\text{cm}^{-1}$ , corresponding to the stretching vibrations of H–O–H bonds; and the band around 1647  $\text{cm}^{-1}$ , which is related to the bending vibration of the –OH groups of the hydrated reaction products associated with H<sub>2</sub>O (Al-Majidi, Lampropoulos et al. 2016). The peak of steam curing around 464.04  $\text{cm}^{-1}$  is assigned to in-plane bending of Si–O and Al–O linkage (Santa, Kessler et al. 2018), while is accompanied by a shift to 465.29, 465.02 and 464.22  $\text{cm}^{-1}$  for ambient, water and temperature curing respectively, can be attributed to the asymmetric stretching of Si–O and Al–O bonds originated from individual tetrahedrals (Phair, Van Deventer et al. 2000, Prasanphan, Wannagon et al. 2019). The band located at 646.76, 647.72, 648.30 and 646.23  $\text{cm}^{-1}$  for temperature, water, ambient and steam curing respectively, is assigned to the tetrahedral group AlO<sub>4</sub> (Ptáček, Šoukal et al. 2011).

The peaks located at 696.87–727.30  $\text{cm}^{-1}$  for water curing, 695.86–727.23  $\text{cm}^{-1}$  for temperature curing, 696.27–727.26  $\text{cm}^{-1}$  for ambient curing and 694.33–727.14  $\text{cm}^{-1}$  for steam curing are attributed to the bending vibration and the symmetric stretching vibration of Al–O–Si (Catauro, Bollino et al. 2014, Chen, Zhou et al. 2018). While, the peaks at 1004.04, 1008.01, 1005.80 and 1003.90  $\text{cm}^{-1}$  are attributed to the asymmetric stretching vibrations of Si–O–T (T = Si or Al) for temperature, water, ambient and steam curing respectively, is shown in Fig. 3 (Lo, Lin et al. 2017). Bands arising at 1476.01, 1476, 1471.40 and 1476.02  $\text{cm}^{-1}$  for temperature, water, ambient and

steam curing respectively, are mainly due to the asymmetric stretching O–C–O bond vibrations in carbonate groups ( $\text{CO}_3^{2-}$ ), which is a result of alkaline metal hydroxide reacting with atmospheric  $\text{CO}_2$  (Li, Rao et al. 2018). The peak at  $1647.23 \text{ cm}^{-1}$  and  $3468.84 \text{ cm}^{-1}$  corresponds to the stretching and deformation vibration modes of H–O–H and O–H, respectively. Thus, this indicates that the reaction product is dominated by chain-structured C–A–S–H and N–A–S–H gels. From the aspect of starting materials, the Si–O bond in sample steam curing that is independent of the ratio of slag is around  $1003.90 \text{ cm}^{-1}$ . The increase in wavenumber shows the formation of more polymerized Si–O network.

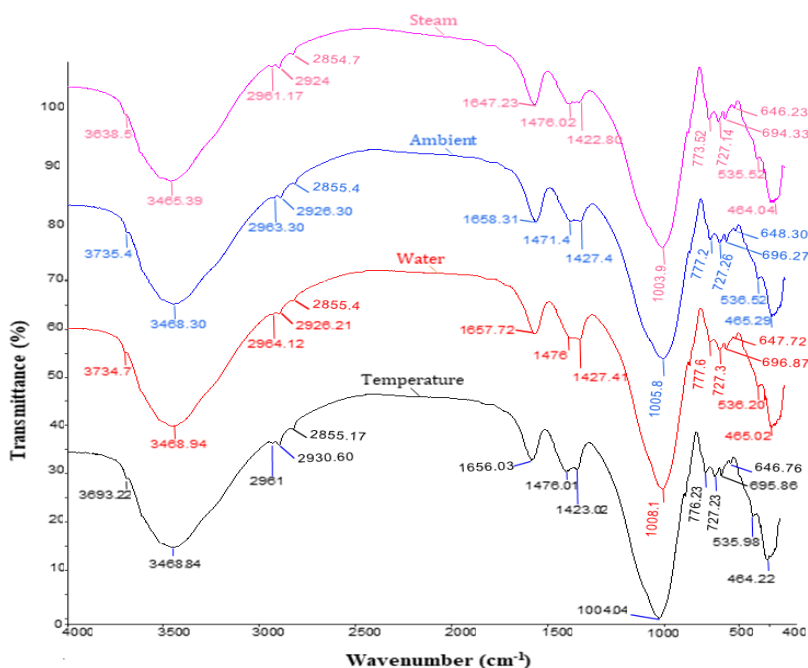


FIGURE 3. FTIR spectra of AATM mixtures at 28 days.

#### 4. Conclusions

This study experimentally investigated the feasibility of compressive strength (CS) development of AATM using sources materials

UPOFA, MK, and GGBFS, cured at different curing conditions. The results showed that the CS and the microstructure of ternary blended AAMs are greatly influenced by curing temperatures and steam curing. Although the chemical composition of geopolymers cured at different conditions was not noticeably changed, a clear difference was observed in the CS. For example, when the samples were steam curing for 28 d compressive strengths increased and reached 88.89 MPa compared to 70.40 MPa for ambient curing. The formation of N–A–S–H, C–S–H and C–A–S–H due to the presence of MK has a high Al content and GGBFS has a high Ca content that leads to formation this gels binder. The formations are responsible for the high CS of the AATM as indicated by XRD, and FTIR analysis.

### Acknowledgements

The authors gratefully acknowledge the Universiti Sains Malaysia for providing the financial support through the University Bridging Grant (304/PAWAM/6316313) for the undertaking of the research work.

### 5. References

- Al-Majidi, M. H., A. Lampropoulos, A. Cundy and S. Meikle (2016). "Development of geopolymer mortar under ambient temperature for in situ applications." *Construction and Building Materials* **120**: 198-211.
- Ariffin, M., M. Azreen, M. W. Hussin and M. A. Rafique Bhutta (2011). Mix design and compressive strength of geopolymer concrete containing blended ash from agro-industrial wastes. *Advanced Materials Research*, Trans Tech Publ.
- Assi, L. N., E. E. Deaver and P. Ziehl (2018). "Effect of source and particle size distribution on the mechanical and microstructural properties of fly Ash-Based geopolymer concrete." *Construction and Building Materials* **167**: 372-380.
- Borges, P. H., V. A. Nunes, T. H. Panzera, G. Schileo and A. Feteira (2016). "The influence of rice husk ash addition on the properties of metakaolin-based geopolymers." *The Open Construction and Building Technology Journal* **10**(1): 406-417.

- C109/C109M, A. (1999). Standard Test Method for Compressive Strength of Hydraulic Cement Mortars (Using 2-in. or [50-mm] Cube Specimens), ASTM International West Conshohocken, Pa.
- Catauro, M., F. Bollino, F. Papale and G. Lamanna (2014). "Investigation of the sample preparation and curing treatment effects on mechanical properties and bioactivity of silica rich metakaolin geopolymer." *Materials Science and Engineering: C* **36**: 20-24.
- Chen, X., M. Zhou, W. Shen, G. Zhu and X. Ge (2018). "Mechanical properties and microstructure of metakaolin-based geopolymer compound-modified by polyacrylic emulsion and polypropylene fibers." *Construction and Building Materials* **190**: 680-690.
- Chindaprasirt, P., P. De Silva, K. Sagoe-Crentsil and S. Hanjitsuwan (2012). "Effect of SiO<sub>2</sub> and Al<sub>2</sub>O<sub>3</sub> on the setting and hardening of high calcium fly ash-based geopolymer systems." *Journal of materials science* **47**(12): 4876-4883.
- Davidovits, J. (2008). *Geopolymer chemistry and applications*, Geopolymer Institute.
- De Silva, P. and K. Sagoe-Crenstil (2008). "Medium-term phase stability of Na<sub>2</sub>O–Al<sub>2</sub>O<sub>3</sub>–SiO<sub>2</sub>–H<sub>2</sub>O geopolymer systems." *Cement and Concrete Research* **38**(6): 870-876.
- Duxson, P., J. L. Provis, G. C. Lukey, S. W. Mallicoat, W. M. Kriven and J. S. J. van Deventer (2005). "Understanding the relationship between geopolymer composition, microstructure and mechanical properties." *Colloids and Surfaces A: Physicochemical and Engineering Aspects* **269**(1): 47-58.
- Fardjaoui, N.-E.-H., B. Wicklein, P. Aranda, I. Sobrados, F. Z. El Berrichi and E. Ruiz-Hitzky (2018). "Modulation of inorganic matrices for functional nanoarchitectures fabrication: The simultaneous effect of moisture and temperature in the preparation of metakaolin based geopolymers." *Bulletin of the Chemical Society of Japan* **91**(7): 1158-1167.

- Gao, X., Q. L. Yu and H. J. H. Brouwers (2015). "Properties of alkali activated slag-fly ash blends with limestone addition." *Cement and Concrete Composites* **59**: 119-128.
- García-Lodeiro, I., A. Fernández-Jiménez, A. Palomo and D. E. Macphee (2010). "Effect of calcium additions on N-A-S-H cementitious gels." *Journal of the American Ceramic Society* **93**(7): 1934-1940.
- Granizo, M. L., S. Alonso, M. T. Blanco-Varela and A. Palomo (2002). "Alkaline activation of metakaolin: effect of calcium hydroxide in the products of reaction." *Journal of the American Ceramic Society* **85**(1): 225-231.
- He, P., M. Wang, S. Fu, D. Jia, S. Yan, J. Yuan, J. Xu, P. Wang and Y. Zhou (2016). "Effects of Si/Al ratio on the structure and properties of metakaolin based geopolymer." *Ceramics international* **42**(13): 14416-14422.
- Huseien, G. F., M. Ismail, M. M. Tahir, J. Mirza, N. H. A. Khalid, M. A. Asaad, A. A. Husein and N. N. Sarbini (2018). "Synergism between palm oil fuel ash and slag: Production of environmental-friendly alkali activated mortars with enhanced properties." *Construction and Building Materials* **170**: 235-244.
- Huseien, G. F., A. R. M. Sam, K. W. Shah, M. A. Asaad, M. M. Tahir and J. Mirza (2019). "Properties of ceramic tile waste based alkali-activated mortars incorporating GBFS and fly ash." *Construction and Building Materials* **214**: 355-368.
- Krivenko, P. V. (1994). "Alkaline cements." *Proceedings of the 1st International Conference on Alkaline Cements and Concretes, Kiev, Ukraine, 1994* **1**: 11-129.
- Kumar, S., R. Kumar and S. Mehrotra (2010). "Influence of granulated blast furnace slag on the reaction, structure and properties of fly ash based geopolymer." *Journal of materials science* **45**(3): 607-615.
- Kupwade-Patil, K. and E. N. Allouche (2012). "Impact of alkali silica reaction on fly ash-based geopolymer concrete." *Journal of materials in Civil Engineering* **25**(1): 131-139.
- Li, X., F. Rao, S. Song, M. A. Corona-Arroyo, N. Ortiz-Lara and E. A. Aguilar-Reyes (2018). "Effects of aggregates on the

- mechanical properties and microstructure of geothermal metakaolin-based geopolymers." *Results in Physics* **11**: 267-273.
- Liew, Y., H. Kamarudin, A. M. Al Bakri, M. Bnhussain, M. Luqman, I. K. Nizar, C. Ruzaidi and C. Heah (2012). "Optimization of solids-to-liquid and alkali activator ratios of calcined kaolin geopolymeric powder." *Construction and Building Materials* **37**: 440-451.
- Lizcano, M., A. Gonzalez, S. Basu, K. Lozano and M. Radovic (2012). "Effects of water content and chemical composition on structural properties of alkaline activated metakaolin-based geopolymers." *Journal of the American Ceramic Society* **95**(7): 2169-2177.
- Lo, K.-W., K.-L. Lin, T.-W. Cheng, Y.-M. Chang and J.-Y. Lan (2017). "Effect of nano-SiO<sub>2</sub> on the alkali-activated characteristics of spent catalyst metakaolin-based geopolymers." *Construction and Building Materials* **143**: 455-463.
- Megat Johari, M. A., A. M. Zeyad, N. Muhamad Bunnori and K. S. Ariffin (2012). "Engineering and transport properties of high-strength green concrete containing high volume of ultrafine palm oil fuel ash." *Construction and Building Materials* **30**(0): 281-288.
- Menshaz, A. M., M. A. M. Johari and Z. A. Ahmad (2017). Characterization of metakaolin treated at different calcination temperatures. AIP Conference Proceedings, AIP Publishing.
- Mijarsh, M., M. M. Johari and Z. A. Ahmad (2015). "Effect of delay time and Na<sub>2</sub>SiO<sub>3</sub> concentrations on compressive strength development of geopolymer mortar synthesized from TPOFA." *Construction and Building Materials* **86**: 64-74.
- Mo, K. H., U. J. Alengaram and M. Z. Jumaat (2014). "A review on the use of agriculture waste material as lightweight aggregate for reinforced concrete structural members." *Advances in Materials Science and Engineering* **2014**.

- Nataraja, M. and L. Das (2010). "Concrete Mix Proportioning as per IS 10262: 2009-Comparison with IS 10262: 1982 and ACI 211.1-91." The Indian Concrete Journal: 64-70.
- Phair, J. W., J. Van Deventer and J. Smith (2000). "Mechanism of polysialation in the incorporation of zirconia into fly ash-based geopolymers." Industrial & engineering chemistry research **39**(8): 2925-2934.
- Prasanphan, S., A. Wannagon, T. Kobayashi and S. Jiemsirilers (2019). "Reaction mechanisms of calcined kaolin processing waste-based geopolymers in the presence of low alkali activator solution." Construction and Building Materials **221**: 409-420.
- Ptáček, P., F. Šoukal, T. Opravil, M. Nosková, J. Havlica and J. Brandštetr (2011). "Mid-infrared spectroscopic study of crystallization of cubic spinel phase from metakaolin." Journal of Solid State Chemistry **184**(10): 2661-2667.
- Ranjbar, N., M. Mehrali, A. Behnia, U. J. Alengaram and M. Z. Jumaat (2014). "Compressive strength and microstructural analysis of fly ash/palm oil fuel ash based geopolymer mortar." Materials & Design **59**: 532-539.
- Samet, B. and M. Chaabouni (2004). "Characterization of the Tunisian blast-furnace slag and its application in the formulation of a cement." Cement and Concrete Research **34**(7): 1153-1159.
- Santa, R. A. A. B., J. C. Kessler, C. Soares and H. G. Riella (2018). "Microstructural evaluation of initial dissolution of aluminosilicate particles and formation of geopolymer material." Particuology.
- Sharmin, A., U. J. Alengaram, M. Z. Jumaat, M. O. Yusuf, S. A. Kabir and I. I. Bashar (2017). "Influence of source materials and the role of oxide composition on the performance of ternary blended sustainable geopolymer mortar." Construction and Building Materials **144**: 608-623.
- Singh, B., G. Ishwarya, M. Gupta and S. K. Bhattacharyya (2015). "Geopolymer concrete: A review of some recent developments." Construction and Building Materials **85**: 78-90.

- Stevenson, M. and K. Sagoe-Crentsil (2005). "Relationships between composition, structure and strength of inorganic polymers." *Journal of Materials Science* **40**(8): 2023-2036.
- Tangchirapat, W., T. Saeting, C. Jaturapitakkul, K. Kiattikomol and A. Siripanichgorn (2007). "Use of waste ash from palm oil industry in concrete." *Waste Management* **27**(1): 81-88.
- Tchadjie, L. N. and S. O. Ekolu (2018). "Enhancing the reactivity of aluminosilicate materials toward geopolymer synthesis." *Journal of Materials Science* **53**(7): 4709-4733.
- Wan, Q., F. Rao, S. Song, R. E. García, R. M. Estrella, C. L. Patino and Y. Zhang (2017). "Geopolymerization reaction, microstructure and simulation of metakaolin-based geopolymers at extended Si/Al ratios." *Cement and Concrete Composites* **79**: 45-52.
- Yuan, J., P. He, D. Jia, C. Yang, S. Yan, Z. Yang, X. Duan, S. Wang and Y. Zhou (2016). "Effect of curing temperature and SiO<sub>2</sub>/K<sub>2</sub>O molar ratio on the performance of metakaolin-based geopolymers." *Ceramics International* **42**(14): 16184-16190.
- Yusuf, M. O., M. A. Megat Johari, Z. A. Ahmad and M. Maslehuddin (2014). "Evolution of alkaline activated ground blast furnace slag-ultrafine palm oil fuel ash based concrete." *Materials & Design* **55**(0): 387-393.
- Zhang, B., P. Yuan, H. Guo, L. Deng, Y. Li, L. Li, Q. Wang and D. Liu (2021). "Effect of curing conditions on the microstructure and mechanical performance of geopolymers derived from nanosized tubular halloysite." *Construction and Building Materials* **268**: 121186.